APPLICATION OF HIGH-ORDER UPWIND DISCRETIZATIONS FOR CALCULATING INCOMPRESSIBLE FLUID FLOWS

A.C. Brandi
Departamento de Computação e Estatística, ICMC, USP, 13560-970 São Carlos, SP, Brasil.
analice@lcad.icmc.usp.br

V.G. Ferreira
Departamento de Computação e Estatística, ICMC, USP, 13560-970 São Carlos, SP, Brasil.
pvgf@lcad.icmc.usp.br

J.A. Cuminato
Departamento de Computação e Estatística, ICMC, USP, 13560-970 São Carlos, SP, Brasil.
jacumina@lcad.icmc.usp.br

A. Castelo
Departamento de Computação e Estatística, ICMC, USP, 13560-970 São Carlos, SP, Brasil.
castelo@lcad.icmc.usp.br

M.F. Tomé
Departamento de Computação e Estatística, ICMC, USP, 13560-970 São Carlos, SP, Brasil.
murilo@lcad.icmc.usp.br

Abstract. *Modern high-order upwind schemes are included into the Freeflow-2D code for the numerical solution of 2D unsteady advection-dominated incompressible flows. Together with appropriate initial and boundary conditions, the Navier-Stokes equations are solved by using the finite difference method. In order to demonstrate the capabilitity of the current code, results for channel flow, flow over a backward facing step and jet impinging onto a solid surface are presented.*

Keywords: *High-Order Upwind, Free Surface Flows, VONOS, WACEB, CUBISTA*

1. Introduction

Nowadays there is a considerable increased effort in developing and applying discretization methods for convective terms of advection-dominated fluid transport equations. In general, these approximation greatly affects the stability and accuracy of the overall numerical method. On the one hand, the first-order upwinding scheme is one of the most appropriate to smooth out oscilations/instabilities, but it is highly diffusive since the spacial second-order derivative in the truncation error competes with any physical diffusion. On the other hand, the usual second-order central differece and QUICK (Quadratic Upstream Interpolation for Convective Kinematics) schemes are plagued by oscillations/instabilities. In order to minimize the numerical physical diffusion effect and, at the same time, to obtain oscillation/instability free approximations, it is essential to adopt a strategy to discretize the convective terms that combines first and high-order discretization and takes into account the propagation of physical information. The results of this composition are the high-order bounded upwind techniques.

In the past few decades, a number of high-order upwinding strategies have been proposed to overcome these difficulties, being that the combination of NVD (Normalised Variable Diagram) [9] and TVD (Total Variation Diminishing) [7] is one of the most popular. In 1998, Varonos and Bergeles [15] proposed the VONOS (Variable-Order Non-Oscillatory Scheme) NVD scheme for which emerged, according to Ferreira et al. [5], as an acceptable upwinding method for simulation of free surface flows. Song et al [12], in 2000, proposed a third-order accurate and limited scheme named WACEB (Weighted-Average Coefficient Ensuring Boundedness) TVD. Numerical results for scalar convection problems show that this scheme has the ability of the QUICK in reducing numerical diffusion without introducing oscillations. However, this scheme still has convergence problems for some non-newtonian flows. As a remedy, in 2003, Alves et al. [1] devised a high-resolution scheme named CUBISTA (Convergent and Universally Bounded Interpolation Scheme for Treatment of Advection) TVD, which is associated with the Courant number. The evaluation of the accuracy and convergence properties of the scheme was measured in two dimensional cases by using linear and non-linear problems and involving newtonian and non-newtonian fluid flows.

In the present study, the *Freeflow-2D* [11] code is used to solve the unsteady incompressible Navier-Stokes equation for advection-dominated confined/free surface fluid flow problems. For this, the VONOS, WACEB and CUBISTA schemes are employed to discretize the non-linear terms. The capabilitity of the current code is then assessed by using channel

flow, flow over a backward facing step and jet impinging onto a rigid wall.

2. Working Equations

The flow is assumed to be unsteady, newtonian and 2D incompressible. The non-dimensional continuity and momentum equations are, respectively,

$$\nabla \cdot \mathbf{u} = 0, \tag{1}$$

$$\frac{\partial \mathbf{u}}{\partial t} + \nabla \cdot (\mathbf{uu}) = -\nabla p + \frac{1}{Re}\nabla^2 \mathbf{u} + \frac{1}{Fr^2}\mathbf{g}, \tag{2}$$

where t is time, $\mathbf{g}$ is the gravitational field, $\mathbf{u}(\mathbf{x},t) = (u(\mathbf{x},t), v(\mathbf{x},t))$ is the vector of fluid velocity in the x and y directions, respectively, and p is the pressure. $Re = (LU)/\nu$ e $Fr = U/(\sqrt{L|\mathbf{g}|})$ are, respectively, the Reynolds and Froude numbers, being L and U length and velocity scales, respectively, and ν the kinematic viscosity of the fluid.

Together with initial and boundary condition, equations (1) and (2) are solved using the *Freeflow-2D* code. For initial conditions, all variables are prescribed. On rigid wall, the velocity obeys the no-slip condition ($\mathbf{u} = 0$). At inlet section, it is imposed a parabolic profile for the velocity, and at the outlet section the homogeneous Neumann condition for this variable. By neglecting suface tension effects, the conditions on free surfaces are (see, for example, Tomé et al. [14])

$$p - \frac{2}{Re}\left[\frac{\partial u}{\partial x}n_x^2 + \frac{\partial v}{\partial y}n_y^2 + \left(\frac{\partial u}{\partial y} + \frac{\partial v}{\partial x}\right)n_x n_y\right] = 0, \tag{3}$$

$$\frac{1}{Re}\left[2\frac{\partial u}{\partial x}m_x n_x + 2\frac{\partial v}{\partial y}m_y n_y + \left(\frac{\partial u}{\partial y} + \frac{\partial v}{\partial x}\right)(m_x n_y + m_y n_x)\right] = 0, \tag{4}$$

where m_x and m_y are the components of the tangent vector to the surface, and n_x and n_y are the components of the normal vector to the surface.

3. Numerical Method

The finite-difference approach is used to discretize the working equations. In order to avoid checkerboard solutions, a uniform cartesian staggered grid system is utilized, with scalars (for example, pressure) defined at cell centers and velocities located at the cell faces. For flows possessing free surfaces, the free surface generally moves and therefore the domain of interest deforms with time. In this case, the front-tracking MAC (Marker and Cell) method [6] is adopted in *Freeflow-2D* to determine the free surface location. In summary, the interface is represented discretely by lagrangian markers connected to form a front which lies within and moves through a eulerian mesh; as the front moves and deforms, interface points are added/deleted and reconnected as necessary (for details, see [10]).

To advance the numerical solution in time, the projection method [4] is employed. It is supposed that, at a given time $t = t_0$, the velocity field $\mathbf{u}(x,y,t_0)$ is known and suitable boundary conditions for the velocity and pressure are given. The updated velocity field $\mathbf{u}(x,y,t)$, at $t = t_0 + \delta t$, is calculated as follows:

step 1: Let $\tilde{p}$ be an arbitrary pressure field, which satisfies the correct pressure condition on the free surface. This pressure field is constructed employing the normal-stress condition (3) at the free surface cells, and it is chosen arbitrarily (for instance $\tilde{p} = 0$) at the interior cells;

step 2: Calculate the intermediate velocity field $\tilde{\mathbf{u}}$ from the explicit discretization of

$$\left.\frac{\partial \tilde{\mathbf{u}}}{\partial t}\right|_{t=t_0} = \left\{ - CONV(\mathbf{uu}) - \nabla\tilde{p} + \frac{1}{Re}\nabla^2\mathbf{u} + \frac{1}{Fr^2}\mathbf{g}\right\}\Bigg|_{t=t_0}, \tag{5}$$

with $\tilde{\mathbf{u}} = \mathbf{u}$, using the correct boundary conditions for $\mathbf{u}$. The term $CONV(\mathbf{uu})$ represents the convective term $\nabla \cdot (\mathbf{uu})$. It can be shown that $\tilde{\mathbf{u}}$ possesses the correct vorticity at time t. However, $\tilde{\mathbf{u}}$ does not satisfy Eq. (1). Let

$$\mathbf{u} = \tilde{\mathbf{u}} - \nabla\psi \tag{6}$$

be the updated velocity field at time t, with ψ an auxiliary potential field such that

$$\nabla^2\psi(\mathbf{x},t) = \nabla \cdot \tilde{\mathbf{u}}(\mathbf{x},t). \tag{7}$$

Thus, $\mathbf{u}$ now satisfies (1) and the vorticity remains unchanged;

step 3: Solve the Poisson equation (7);

step 4: Compute the velocity field (6);

step 5: Compute the pressure. It can be shown that the pressure is given by $p = \tilde{p} + \psi/\delta t$;

step 6: Update, in case of free surface flows, the positions of the marker particles. This last step involves moving the marker particles to their new positions. So, the new free surface position is calculated by integrating the ordinary differential equations $\dot{x} = u$ and $\dot{y} = v$ by Euler's method.

In Eq. (5), the viscous terms and the pressure gradient are approximated using standard second-order finite differences, while the temporal derivative is discretized using a forward difference. The Poisson equation (7) is discretized using the usual five-point laplacian operator, and the corresponding symmetric-positive definite linear system is solved by the conjugate-gradient method. In short, the equations (1), (2) and (7) are, respectively, discretized as follow:

$$\frac{u_{i+\frac{1}{2},j} - u_{i-\frac{1}{2},j}}{\delta x} + \frac{v_{i,j+\frac{1}{2}} - v_{i,j-\frac{1}{2}}}{\delta y} = 0,$$

$$\begin{aligned}\tilde{u}^{n+1}_{i+\frac{1}{2},j} &= u^n_{i+\frac{1}{2},j} + \delta t \left\{ CONV(u)\Big|_{i+\frac{1}{2},j} - \frac{\tilde{p}_{i+1,j} - \tilde{p}_{i,j}}{\delta x} \right. \\ &+ \left. \frac{1}{Re}\left(\frac{u_{i-\frac{1}{2},j} - 2u_{i+\frac{1}{2},j} + u_{i+\frac{3}{2},j}}{\delta x^2} + \frac{u_{i+\frac{1}{2},j+1} - 2u_{i+\frac{1}{2},j} + u_{i+\frac{1}{2},j-1}}{\delta y^2} \right) + \frac{1}{Fr^2} g_x \right\}^n,\end{aligned}$$

$$\begin{aligned}\tilde{v}^{n+1}_{i,j+\frac{1}{2}} &= v^n_{i,j+\frac{1}{2}} + \delta t \left\{ CONV(v)\Big|_{i,j+\frac{1}{2}} - \frac{\tilde{p}_{i,j+1} - \tilde{p}_{i,j}}{\delta y} \right. \\ &+ \left. \frac{1}{Re}\left(\frac{v_{i+1,j+\frac{1}{2}} - 2v_{i,j+\frac{1}{2}} + v_{i-1,j+\frac{1}{2}}}{\delta x^2} + \frac{v_{i,j+\frac{3}{2}} - 2v_{i,j+\frac{1}{2}} + v_{i,j-\frac{1}{2}}}{\delta y^2} \right) + \frac{1}{Fr^2} g_y \right\}^n,\end{aligned}$$

$$\frac{\psi_{i+1,j} - 2\psi_{i,j} + \psi_{i-1,j}}{\delta x^2} + \frac{\psi_{i,j+1} - 2\psi_{i,j} + \psi_{i,j-1}}{\delta y^2} = \frac{\tilde{u}_{i+\frac{1}{2},j} - \tilde{u}_{i-\frac{1}{2},j}}{\delta x} + \frac{\tilde{v}_{i,j+\frac{1}{2}} - \tilde{v}_{i,j-\frac{1}{2}}}{\delta y},$$

where the convective terms $CONV(u)$ and $CONV(v)$ in the discretized Navier-Stokes equations are approximated by the high-order upwind VONOS, WACEB and CUBISTA schemes. For simplicity, only the convective term $CONV(u)$ will be presented. The discretization of the other terms is made in the similar manner. In location $(i + \frac{1}{2}, j)$, the term $CONV(u)$ can be aproximated by the following conservative scheme:

$$CONV(u)\Big|_{i+\frac{1}{2},j} \approx \frac{\bar{u}_{i+1,j}u_{i+1,j} - \bar{u}_{i,j}u_{i,j}}{\delta x} + \frac{\bar{v}_{i+\frac{1}{2},j+\frac{1}{2}}u_{i+\frac{1}{2},j+\frac{1}{2}} - \bar{v}_{i+\frac{1}{2},j-\frac{1}{2}}u_{i+\frac{1}{2},j-\frac{1}{2}}}{\delta y},$$

where the convected velocities are obtained by averaging. For instance, $\bar{v}_{i+\frac{1}{2},j-\frac{1}{2}}$ is approximate by

$$\bar{v}_{i+\frac{1}{2},j-\frac{1}{2}} \approx 0.5\left(v_{i,j-\frac{1}{2}} + v_{i+1,j-\frac{1}{2}}\right).$$

The velocities $u_{i,j}$ and $u_{i+1,j}$ are calculated, for example, using the CUBISTA scheme, (the others velocities and schemes follow similar procedures), by

- When $\bar{u}_{i,j} > 0$ and $\hat{u}_{i-\frac{1}{2},j} = \frac{u_{i-(1/2),j} - u_{i-(3/2),j}}{u_{i+(1/2),j} - u_{i-(3/2),j}}$, the value of $u_{i,j}$ is

$$u_{i,j} = \begin{cases} u_{i-\frac{1}{2},j} & \text{se} \quad \hat{u}_{i-\frac{1}{2},j} \notin [0,1], \\ \frac{1}{4}(7u_{i-\frac{1}{2},j} - 3u_{i-\frac{3}{2},j}) & \text{se} \quad 0 < \hat{u}_{i-\frac{1}{2},j} < 3/8, \\ \frac{1}{8}(3u_{i+\frac{1}{2},j} + 6u_{i-\frac{1}{2},j} - u_{i-\frac{3}{2},j}) & \text{se} \quad 3/8 \le \hat{u}_{i-\frac{1}{2},j} \le 3/4, \\ \frac{1}{4}(3u_{i+\frac{1}{2},j} + u_{i-\frac{1}{2},j}) & \text{se} \quad 3/4 < \hat{u}_{i-\frac{1}{2},j} < 1. \end{cases}$$

- When $\bar{u}_{i,j} < 0$ and $\hat{u}_{i+\frac{1}{2},j} = \frac{u_{i+(1/2),j} - u_{i+(3/2),j}}{u_{i-(1/2),j} - u_{i+(3/2),j}}$, the value of $u_{i,j}$ is

$$u_{i,j} = \begin{cases} u_{i+\frac{1}{2},j} & \text{se} \quad \hat{u}_{i+\frac{1}{2},j} \notin [0,1], \\ \frac{1}{4}(7u_{i+\frac{1}{2},j} - 3u_{i+\frac{3}{2},j}) & \text{se} \quad 0 < \hat{u}_{i+\frac{1}{2},j} < 3/8, \\ \frac{1}{8}(3u_{i-\frac{1}{2},j} + 6u_{i+\frac{1}{2},j} - u_{i+\frac{3}{2},j}) & \text{se} \quad 3/8 \le \hat{u}_{i+\frac{1}{2},j} \le 3/4, \\ \frac{1}{4}(3u_{i-\frac{1}{2},j} + u_{i+\frac{1}{2},j}) & \text{se} \quad 3/4 < \hat{u}_{i+\frac{1}{2},j} < 1. \end{cases}$$

- When $\bar{u}_{i+1,j} > 0$ and $\hat{u}_{i+\frac{1}{2},j} = \frac{u_{i+(1/2),j} - u_{i-(1/2),j}}{u_{i+(3/2),j} - u_{i-(1/2),j}}$, the value of $u_{i+1,j}$ is

$$u_{i+1,j} = \begin{cases} u_{i+\frac{1}{2},j} & \text{se} \quad \hat{u}_{i+\frac{1}{2},j} \notin [0,1], \\ \frac{1}{4}(7u_{i+\frac{1}{2},j} - 3u_{i-\frac{1}{2},j}) & \text{se} \quad 0 < \hat{u}_{i+\frac{1}{2},j} < 3/8, \\ \frac{1}{8}(3u_{i+\frac{3}{2},j} + 6u_{i+\frac{1}{2},j} - u_{i-\frac{1}{2},j}) & \text{se} \quad 3/8 \le \hat{u}_{i+\frac{1}{2},j} \le 3/4, \\ \frac{1}{4}(3u_{i+\frac{3}{2},j} + u_{i+\frac{1}{2},j}) & \text{se} \quad 3/4 < \hat{u}_{i+\frac{1}{2},j} < 1. \end{cases}$$

- When $\bar{u}_{i+1,j} < 0$ and $\hat{u}_{i+\frac{3}{2},j} = \frac{u_{i+(3/2),j} - u_{i+(5/2),j}}{u_{i+(1/2),j} - u_{i+(5/2),j}}$, the value of $u_{i+1,j}$ is

$$u_{i+1,j} = \begin{cases} u_{i+\frac{3}{2},j} & \text{se} \quad \hat{u}_{i+\frac{3}{2},j} \notin [0,1], \\ \frac{1}{4}(7u_{i+\frac{3}{2},j} - 3u_{i+\frac{5}{2},j}) & \text{se} \quad 0 < \hat{u}_{i+\frac{3}{2},j} < 3/8, \\ \frac{1}{8}(3u_{i+\frac{1}{2},j} + 6u_{i+\frac{3}{2},j} - u_{i+\frac{5}{2},j}) & \text{se} \quad 3/8 \leq \hat{u}_{i+\frac{3}{2},j} \leq 3/4, \\ \frac{1}{4}(3u_{i+\frac{1}{2},j} + u_{i+\frac{3}{2},j}) & \text{se} \quad 3/4 < \hat{u}_{i+\frac{3}{2},j} < 1. \end{cases}$$

4. Numerical Results

The validity of the current *Freeflow-2D* code in simulating complex righ-Reynolds number flows is assessed in this section. We report the numerical results for a channel flow, flow over a backward-facing step and a jet impinging onto a flat surface.

4.1 Channel Flow

In order to verificate the numerical method, we compare the exact [3] and the approximate solutions of the flow of a fluid ($\nu = 0.001\text{m}^2/\text{s}$) between two parallel plates. In this test case, it is considered two parallel plates separated by a distance $L = 1\text{m}$. The Reynolds number was 1.0×10^3, and the computations were performed on three different meshes, namely: the coarse (50×10 computational cells, $\delta x = \delta y = 0.1$ m); the medium (100×20 computational cells, $\delta x = \delta y = 0.05$ m); and the fine (200×40 computational cells, $\delta x = \delta y = 0.025$ m) meshes. The numerical solutions are shown at the middle of the channel ($x = 2.5L$). The length of the channel model used in the simulations was $5L$. The *Freeflow-2D* code equiped with VONOS, WACEB and CUBISTA advection schemes was applied, and the time simulation used for each scheme was $t = 1000$s. The Fig. 1 depicts the comparison between the numerical solution with the CUBISTA scheme and the exact solution. Although we haven't showed here, the comparisons between the numerical and exact solutions using VONOS and WACEB schemes were, approximately, the same as that by CUBISTA. It can be observed from this figure that the numerical results, on the three meshes, are in good agreement with the analytical solution. In fact, the relative l_2-norm of the error is displayed in Table 1. We can see from this table that the errors decrease with mesh refinement. These results demonstrate the convergence of the numerical method presented in this work.

Table 1. Results of error (E_{rel}) for plane channel flow with $Re = 1.0 \times 10^3$ and on three meshes.

mesh	CUBISTA	WACEB	VONOS
coarse	1.2558×10^{-5}	1.2579×10^{-5}	1.2609×10^{-5}
medium	1.0573×10^{-6}	1.0571×10^{-6}	1.0572×10^{-6}
fine	6.9796×10^{-8}	6.9791×10^{-8}	6.9758×10^{-8}

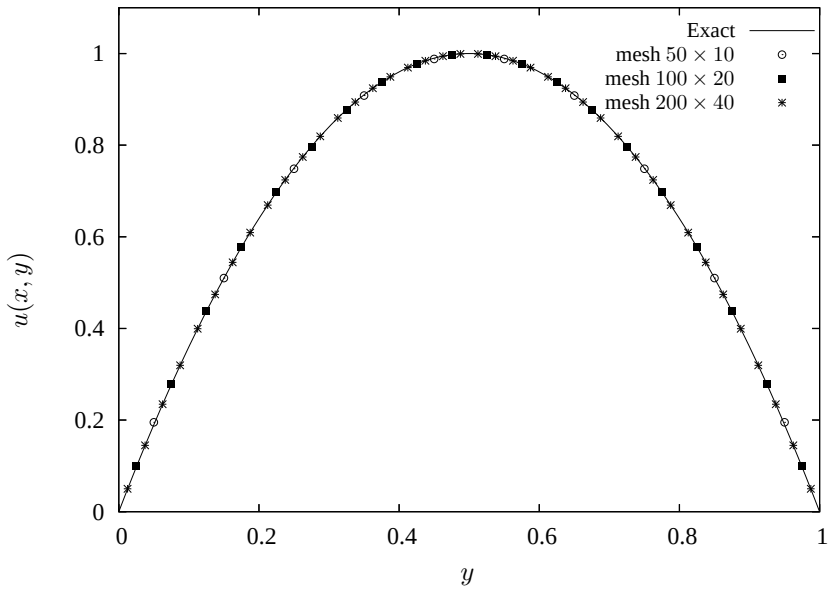

Figure 1. Comparison between numerical solutions obtained with CUBISTA scheme and analytical solution by Batchelor over three meshes and $Re = 1.0 \times 10^3$.

4.2 Flow over a Backward-Facing Step

Flow separation and recirculation caused by a sudden expansion in a channel appear in many engineering applications. Heat exchangers, industrial ducts and flow around buildings are good examples. This flow problem was chosen as a representative test bed because there are in the literature many data, both numerical and experimental. By using the *Freeflow-2D* code, adapted with VONOS, WACEB and CUBISTA convection schemes and a fully developed parabolic velocity profile prescribed at the inlet section, we simulate numerically this fluid flow problem for a wide range o Reynolds numbers. These are based on the maximum velocity $U_{max} = 1.0$m/s at that section and the height of the step h ($h = 0.1$m here). Table 1 shows values of the reattachment length x_1 obtained by experimental/numerical data of Armaly et al. [2], numerical data of Stuart & Dochan [13] and numerical results of *Freeflow-2D*. From this table, one can see that WACEB and CUBISTA schemes provided good results, while VONOS scheme gives worse results. In particular, Fig. 2 grafically depicts a plot of reattachment lengths x_1 against Reynolds numbers using the data of Armaly et al. and Stuart & Dochan and the results with CUBISTA. And, once more, this comparison shows a good agreement between the data for $0 < Re < 400$. Also, one can see from this same figure that for $Re \geq 400$ the numerical results given poor agreement; and this can be explained by the tridimensional effects and, possibly, the turbulence transition in this high Reynolds number problem.

In adition, with the CUBISTA scheme and Reynolds number 266, a convergence test of the numerical solution was performed on three uniform meshes consisting of 175×10, 350×20 and 700×40 cells. This is ilustrated in Fig. 3, which shows how the reattachment length was estimated (the change in the signal of the u velocity component).

Table 2. Estimates for the reattachment length.

Re	**Experimental**	**Numerical**		***Freeflow-2D***		
	Armaly et. al	**Armaly et. al**	**Stuart & Dochan**	**CUBISTA**	**VONOS**	**WACEB**
100	3.06	2.95	2.86	3.13	3.18	3.28
200	5.16	4.82	4.97	5.14	5.14	5.15
400	8.72	8.04	8.03	8.24	8.16	8.20
600	11.28	8.18	10.25	9.71	9.55	9.80
800	14.34	7.50	11.47	10.68	10.62	10.80

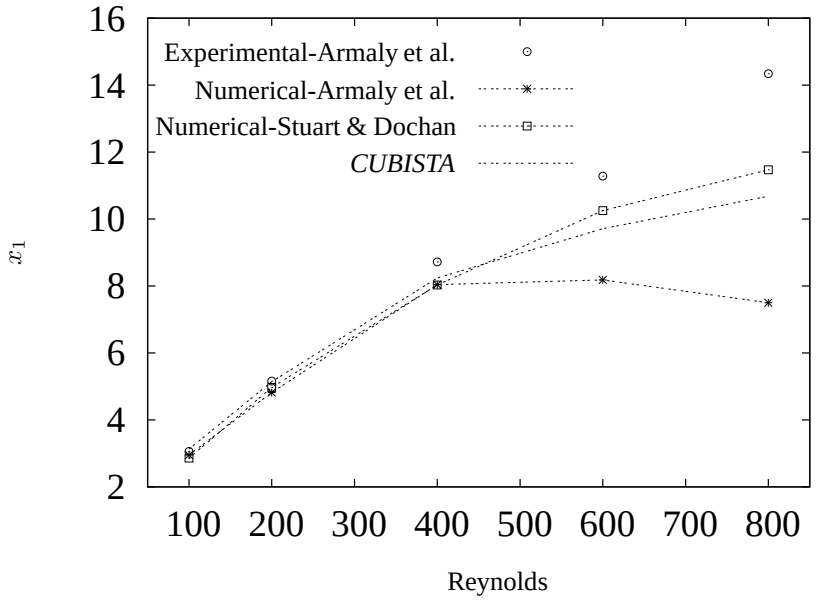

Figure 2. Comparison between experimental data and numerical results.

4.3 Jet Impinging onto a Flat Surface

A jet impinging normally onto flat surface is of great importance in engineering applications. It is, for example, used for enhancing heat transfer devices. This free surface flow was also chosen as a representative test bed because there is

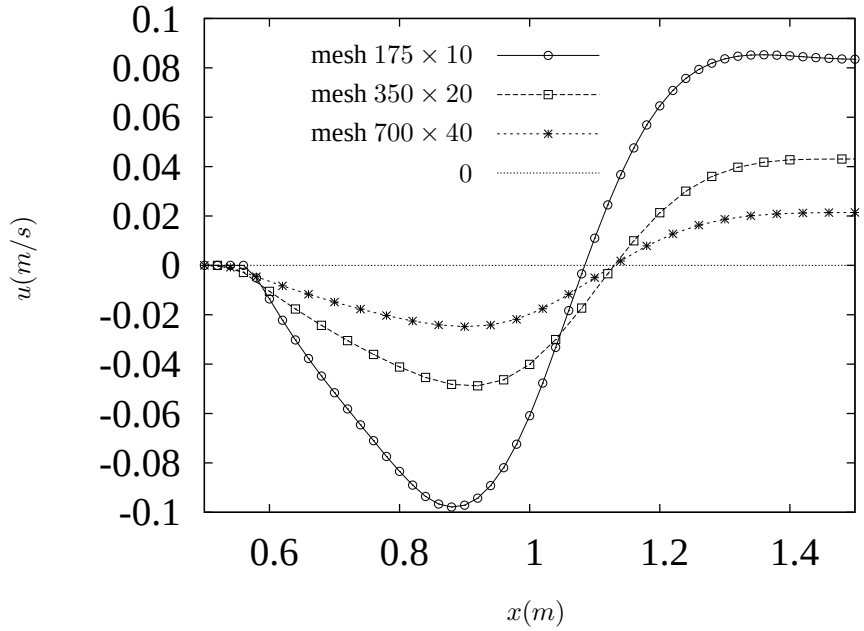

Figure 3. Convergence test of the numerical solution using the CUBISTA scheme at Reynolds number $Re = 266$.

(see [5] and [16]) an analytical solution for the total thickness of the fluid layer flowing on the flat surface. The VONOS, WACEB and CUBISTA convection schemes implemented into the *Freeflow-2D* code were also used to simulate this moving free boundary problem. The Reynolds number based on the maximum velocity $U_{max} = 1.0$m/s and diameter of the inlet ($D = 0.01$m here) was 2000. Using a mesh consisting of 800×80 computational cells, a comparison was made between the free surface height (the total thickness of the layer), obtained from numerical solutions and analytical viscous solution by Watson [16]. This is displayed in Figs. 4, 5 and 6. In particular, Fig. 7 shows the comparison between the three numerical solutions. One can see from these figures that the numerical results obtained with VONOS, WACEB and CUBISTA schemes are very similar, showing in some regions a small difference when compared to the Watson's solution. We believe that most of this difference may be attributed to insufficient grid points used near the rigid wall. In fact, when we refined the mesh (not shown here), the numerical solution converged to a solution close to that obtained with the mesh 800×80 for the three schemes.

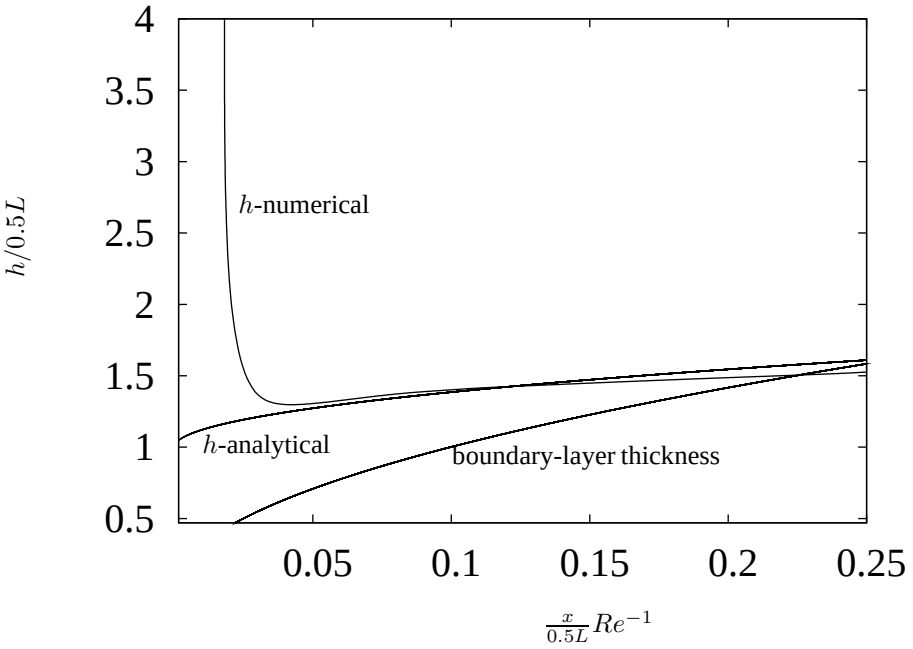

Figure 4. Comparison between numerical solution using VONOS scheme and viscous analytical solution of Watson.

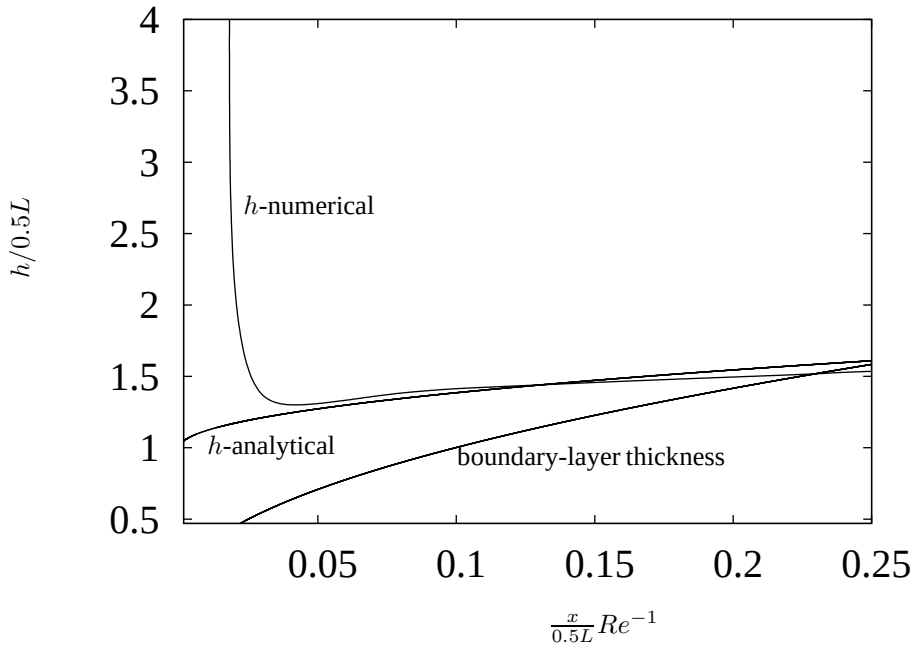

Figure 5. Comparison between numerical solution using WACEB scheme and viscous analytical solution of Watson.

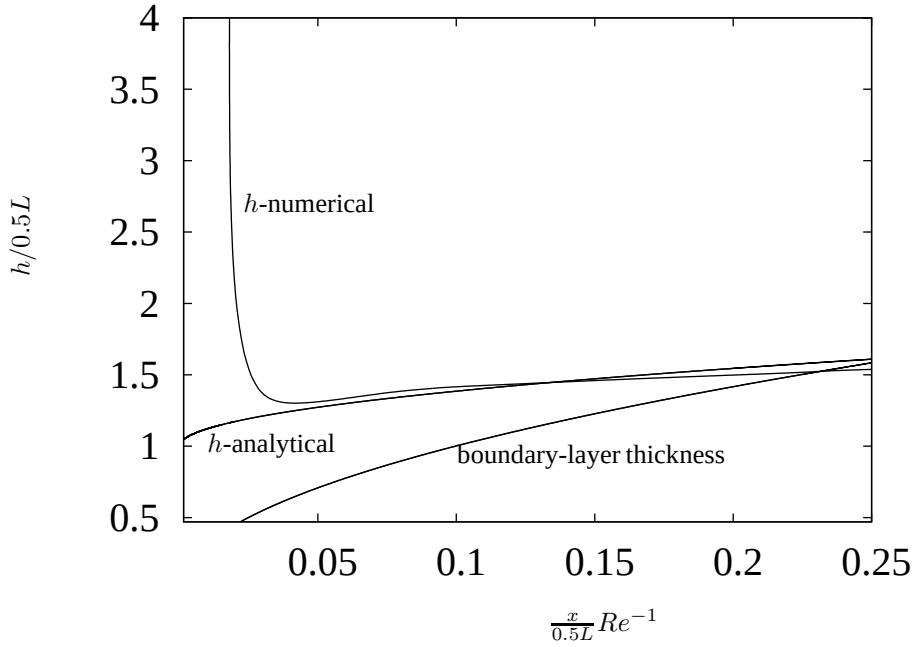

Figure 6. Comparison between numerical solution using CUBISTA scheme and viscous analytical solution of Watson.

5. Concluding Remarks

The high-order VONOS (not TVD), WACEB (TVD) and CUBISTA (TVD) advection schemes have been implemented into the *Freeflow-2D* code for solving 2D advection-dominated incompressible newtonian fluid flow problems. According to the computed results, the new version of the code can, in fact, predict both confined and free surface flows with a satisfactory accuracy.

Particularly, the best upwind schemes emerging from this study are WACEB and CUBISTA. The VONOS scheme presented poor results in case of a flow over a backward-facing step, and we believe that this is because it is not TVD. For the problem of a jet impinging normally onto flat rigid wall, the three schemes show similar results. Although not shown here, the computed results using QUICK and central difference schemes were massacred by oscillations/instabilities.

Future developments include the addition of the $\kappa - \varepsilon$ turbulence model into the *Freeflow-2D* and the inclusion of a

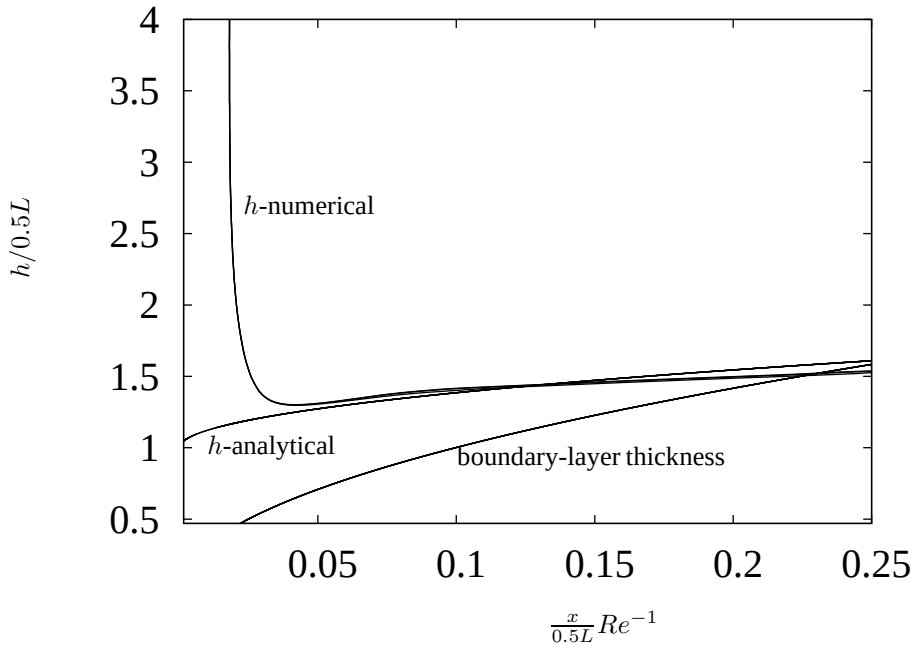

Figure 7. Comparison of the three numerical solution and Watson solution

new adaptative high-order upwinding scheme for numerical solution of laminar/turbulent flows.

6. Acknowledgement

This work was supported by *FAPESP* under Grant No. 02/11774-2.

7. References

Alves, M.A., Oliveira, P.J. and Pinho, F.T., 2003, "A convergent and universally bounded interpolation scheme for the treatment of advection", *Int. J. Numer. Meth. Fluids*, **41**, 47-75.

Armaly, B.F, Durst, F., Periera, J.C.F. and Schönung, B., 1983, "Experimental and theoretical investigation of backward facing step flow", *J. Fluid Mechs.*, **127**, 473.

Batchelor, G.K., 1970, "An introduction to fluid dynamics", Cambridge.

Chorin, A., 1967, "A numerical method for solving incompressible viscous flow problems", *J. Comp. Physics.*, **2**, 12-26.

Ferreira, V.G., Tomé, M.F., Mangiavacchi, N., Castelo, A., Cuminato, J.A., Fortuna, A.O. and McKee, S., 2002, " High order upwinding and the hydraulic jump", *Int. J. Numer. Meth. Fluids*, **39**, 549-583.

Harlow, F.H. and Welch, J.E., 1965, "Numerical calculation of time-dependent viscous incompressible flow of fluid with a free surface" *Physics of Fluids*, **8**, 2182-2189.

Harten A., 1984, "On a class of high resolution total-variation-stable finite-difference schemes". SIAM Journal of Numerical Analysis, **21**, No. 1, 1-23.

Hirsch, C., 1990, "Computational methods for inviscid and viscous flows. Numerical computation of internal and external flows", Vol. 2, John Wiley, New Yok.

Leonard B. P. 1988, "Simple high-accuracy resolution program for convective modelling of discontinuities". International Journal for Numerical Methods in Fluids, **8**, 1291-1318.

McKee, S., Tomé, M.F., Cuminato, J.A., Castelo, A. and Ferreira, V.G., 2004, "Recent advances in the Marker and Cell method", Archives of Computational Methods in Engineering, **11**, 107-142.

Oliveira, J., 1999, "Desenvolvimento de um Sistema de Simulação de Escoamentos de Fluidos com Superfícies Livres Bidimensionais", Dissertação de Mestrado, ICMC, USP, São Carlos, SP.

Song, B., Liu, G.R., Lam, K.Y. and Amano, R.S., 2000, " On a higher-order bounded discretization scheme", *Int. J. Numer. Meth. Fluids*, **32**, 881-897.

Stuart, E.R. and Dochan, K., 1991, "An upwind differencing scheme for the incompressible Navier-Stokes equations", *Appl. Numer. Math.*, **8**, 43-64.

Tomé, M.F. and McKee, S., 1994, "GENSMAC: a computational marker-and-cell method for free surface flows in general domains", *J. Comp. Physics.*, **110**, 171-186.

Varonos, A. and Bergeles, G., 1998, "Development and assessment of a variable-order non-oscillatory for convection term discretization", *Int. J. Numer. Meth. Fluids*, **26**, 1-16.

Watson, E.J., 1964, "The radial spread of a liquid jet over a horinzontal plane", *J. Fluid Mechs.*, **20**, 481-499.

8. Responsibility notice

The authors are the only responsible for the printed material included in this paper